RCC Plug Repair Thermal Tools for Shuttle Mission Support

Alvaro C. Rodriguez and Brian P. Anderson, NASA Johnson Space Center

A thermal math model for the Space Shuttle Reinforced Carbon-Carbon (RCC) Plug Repair was developed to increase the confidence in the repair entry performance and provide a real-time mission support tool. The thermal response of the plug cover plate, local RCC, and metallic attach hardware can be assessed with this model for any location on the wing leading edge. The geometry and spatial location of the thermal mesh also matches the structural mesh which allows for the direct mapping of temperature loads and computation of the thermoelastic stresses. The thermal model was correlated to a full scale plug repair radiant test. To utilize the thermal model for flight analyses, accurate predictions of protuberance heating were required. Wind tunnel testing was performed at CUBRC to characterize the heat flux in both the radial and angular directions. Due to the complexity of the implementation of the protuberance heating, an intermediate program was developed to output the heating per nodal location for all OML surfaces in SINDA format. Three Design Reference Cases (DRC) were evaluated with the correlated plug thermal math model to bound the environments which the plug repair would potentially be used.

Introduction

The Shuttle Orbiter Leading Edge Structural Subsystem is comprised of 101 RCC components that are generally identified as the nose cap, chin panel, wing leading edge (WLE) and arrowhead. RCC is a load-bearing, carbon-based composite thermal protection material capable of operating effectively at temperatures in excess of 3000°F. Because the system is carbon based, it is subject to oxidation at these elevated temperatures. Severe oxidation and subsequent burn-through of an RCC part occurring during entry could lead to the catastrophic loss of crew and vehicle.

The RCC plug repair system, shown in Figure 1, has been developed in order to repair the WLE in the event of potentially catastrophic damage caused by ascent or micro-meteoroid orbital debris. The plug material consists of a C/SiC composite with a SiC coating. An additional coating, MCM-700, is also used to increase oxidation protection of the system and is brushed over the SiC coating. A mechanical titanium zirconium molybdenum (TZM) system is used to conform and attach the flexible C/SiC plug to the RCC curved surface.

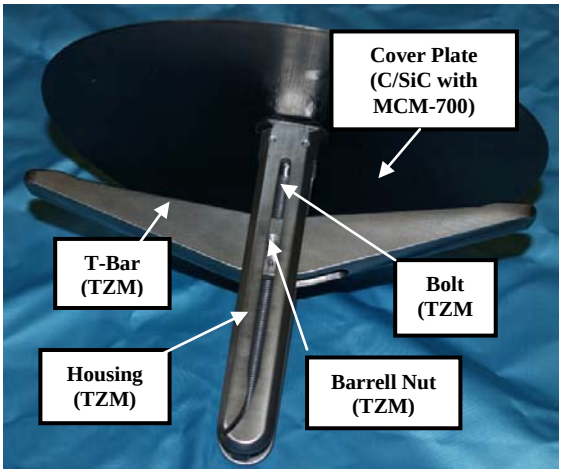

Figure 1: RCC Plug Repair Components

As part of the effort to establish confidence in the RCC plug repair system, thermo-structural models have been developed to predict its performance during re-entry. Thermal models were developed to predict the peak temperatures on the RCC and repair components to evaluate whether the materials will exceed their temperature limits as well as map the temperature loads onto the stress model. These predictions are also required to be efficient to support real-time mission support timelines.

Thermal Model

The plug repair thermal math model (TMM) was based on the geometry and mesh developed at ATK Thiokol as part of the thermo-structural analysis study.[(1)] However, the ATK mesh utilized 20-node brick elements and, when imported into Thermal Desktop®, was simplified into 4-node brick elements since the original 20-node brick elements were not supported. More importantly, the geometry between the structural mesh and the newly imported thermal mesh remained consistent for future thermo-structural analyses. Each component of the C/SiC cover plate and TZM attach hardware has a separate mesh and are retained on separate layers for additional control. In total the model contains 12,995 nodes and 14,624 elements. Though the geometry and mesh were derived from the ATK thermal model, the thermal network was completely reestablished in Thermal Desktop® with the focus on creating a real-time mission support model. The thermal and optical properties for RCC, C/SiC, and TZM were obtained from the manufacturers and testing at NASA. Properties were assumed constant at temperatures above the last available data point.

In an effort to reduce the complexity of the ATK thermal model and provide a means to analyze different RCC wing locations, only a 10” x 10” section of the curved RCC region was kept. Figure 2 shows the complete thermal model.

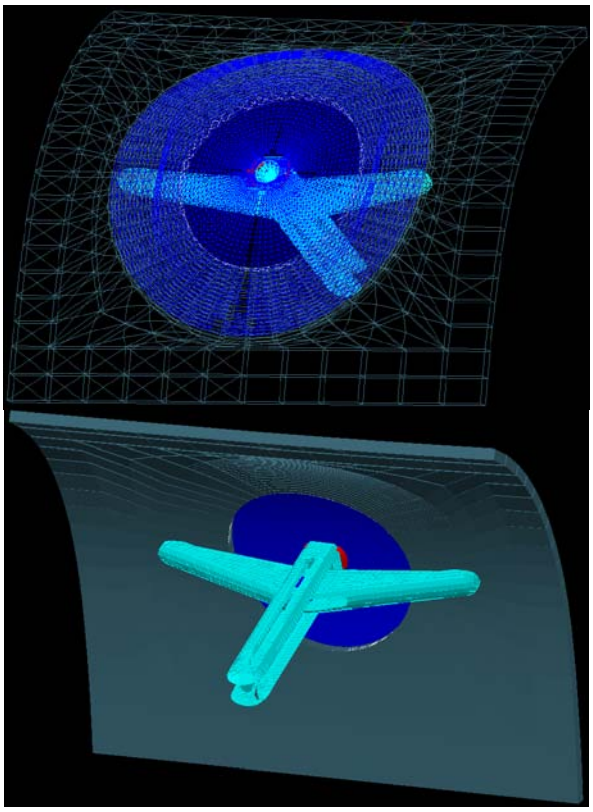

Figure 2: Plug Repair TMM

As part of the real-time mission support, it was desired to evaluate multiple RCC hole configurations. The original mesh was developed to assess a 4in. hole. In order to accommodate additional hole sizes, the inner walls of the original 4 in. hole were extruded to provide a 2 in. and 3 in. hole configuration and assigned the RCC properties. The outer edge of the 2in. and 3in. hole meshes were then merged with the 4in. hole inner nodes to ensure continuity of RCC material. The 2 in. and 3in. holes are contained within separate submodels that can be included in the SINDA build statement to be engaged in the thermal analysis.

Radiative heat transfer is considered on both the external and internal environments. The external surfaces utilize temperature varying optical properties with an assumed 80°F external sink node. This is implemented via a difference conductor based on the temperature difference between the sink node and the nodal temperature of the repair material. A view factor to space of 1.0 is used for the outer mold line (OML) surfaces except for the thin edge of the C/SiC cover plate. A view factor of 0.7 is applied to the C/SiC edge conductor based on an independent Monte Carlo radiation assessment of this configuration, and represents the average view factor result over the edge surface. As part of the standard plug repair procedure, the bolt head is covered with NOAX as an additional barrier to the flow and is modeled by applying a temperature dependent NOAX emissivity property to the bolt head surface.

Monte Carlo ray tracing techniques were used to define the radiative heat transfer between the internal components due to the complexity of the TZM attach hardware. An internal sink node is used to approximate the internal RCC and insulation surfaces in the wing cavity. The sink node is based on the temperature profile from the Boeing 3-D RCC TMM and is discussed in more detail in the Environments section. For the internal radiation, a constant emissivity for all components is utilized. For RCC and TZM, the lowest emissivity from the temperature-emissivity curve is used. For the C/SiC inner mold line (IML) surfaces, the emissivity is based on correlation to the plug repair radiant test.[2]

Heat transfer between the plug repair components and RCC were modeled using contactors and based on the structural analysis of plug gap height distributions[1]. The contact between the plug and RCC was confined to the outer edges and the location of minimum gap at the mid section.

Contact conditions were also applied to other regions of the model to capture the thermal interactions between the TZM components, RCC and C/SiC. Contact regions include : barrel nut to housing, barrel nut to bolt threads, bolt head to plug inner diameter (ID), housing to plug boss, housing to bolt, t-bar to RCC plate and t-bar to barrel nut. The contact conductance values were determined through model correlation with the plug radiant test.

Environments

A set of design reference cases (DRC) were developed for the RCC repair team to capture a range of environments which would build confidence in the repair concepts through testing and analysis for damages at specific locations on the vehicle.[3] The DRCs consist of BP 5505 (Panel 9 stagnation region), nose cap (a superposition of BP 110 and 112), and BP 5951 (Panel 18 upper apex region). Though the DRCs were primarily developed for a separate RCC crack repair project, they have been adapted for the plug repair. The primary difference is that the plug repair cannot be used on the nose cap. So, an equivalent environment on the wing leading edge was developed. In place of the nose cap, an equivalent temperature was found on the wing leading edge on the Panel 8 lower surface. The temperature and heating environments are shown in Figure 3.

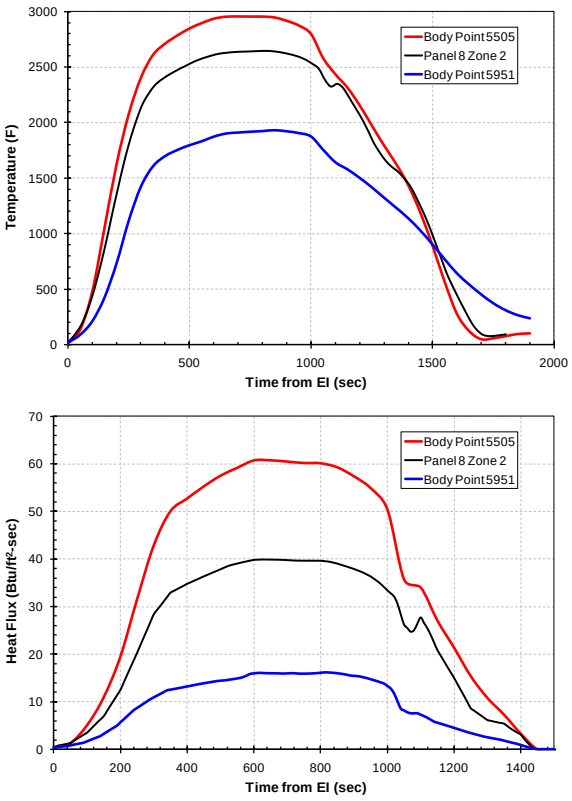

Figure 3: RCC Plug Repair Design Reference Cases

The internal wing cavity environment is important for the radiation exchange. As part of the development of a real-time support tool, the insulation and adjacent RCC boundary surfaces were represented by a sink node for the radiation analyses. This was crucial in developing a time-efficient analysis, though it requires an effective means to verify that the boundary condition simplification provides an adequate representation of the internal environment. To do this, an independent model was developed of the 10" x 10" RCC curved section without damage. By utilizing the nominal heating environments and the removable spar insulation temperature profile, the RCC OML temperature can be predicted and compared to the Boeing 3-D TMM. If the peak temperatures do not match, then the profile can be adjusted iteratively to achieve correlation.

In order to apply the plug thermal model to the flight environment, it was necessary to derive heating on and around the plug hardware. These environments were principally derived from a wind tunnel test performed at CUBRC in Buffalo, NY.[4] The objective of the test was to gather data to validate Computational Fluid Dynamic (CFD) predictions and to examine trends in peak heating and distribution with protuberance height. The data gathered included heat flux from discrete sensors and global infrared temperatures. Discrete sensor placement included several sensors on the leading edge of the plug where peak heating levels were expected as well as sensors around the circumference of the test article. Schlieren images were also obtained to capture flow field patterns. The test conditions were derived to closely match local conditions on the Orbiter on Panel 9 for a Mach 18 trajectory point.

The plug geometry tested was designed and fabricated using plug flight hardware drawings. The diameter of the plug was 7-inches. Step heights of 0.025, 0.045, 0.055, and 0.065-inches were tested. A side-view of the plug test article installed in the tunnel is shown in Figure 4.

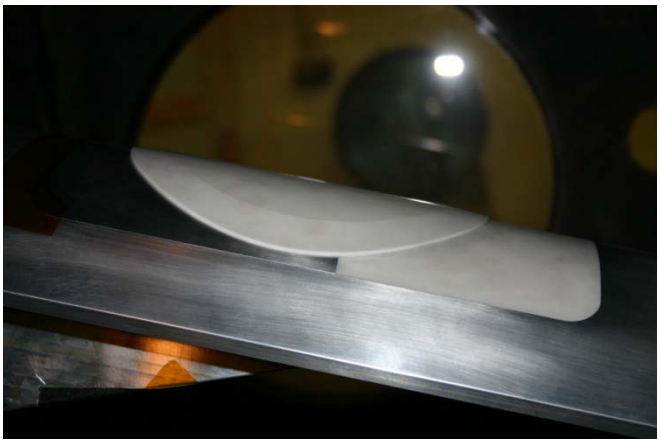

Figure 4: Side-view of plug wind tunnel test model installed in the tunnel

Following the test, the data was examined for trends. Of particular interest was the change in heating levels and heating distribution with the ratio of plug protuberance height (k) to local boundary layer thickness (δ). Empirical heating correlations for the peak heating level and the heating distributions around the circumference of the plug, on the top surface of the plug, and on the front face of the plug were developed by curve fitting the data as a function of k/δ. Additionally, since nominal installation of the plug hardware on the Orbiter would include application of NOAX around the leading edge of the plug, heating adjustments were derived to account for the ramp introduced by the NOAX application.

Application of the heating for the Plug TMM requires a separate application known as the Plug Heating Augmentation Tool v2.3 (PHAT). This program was developed to take in the chordwise heating (spanwise heating is assumed constant over the 10 in. region) and output the heating for the RCC, C/SiC, and Bolt surfaces. The output is formatted to be included in the SINDA block of the CASE SET MANAGER. The augmented heating applied to the C/SiC surfaces is based on the set of engineering correlations derived from CUBRC wind tunnel

test data[5]. The augmented heating is a function of angle to the flow, step height (gap + plug edge thickness, 0.025 in. max.), and boundary layer thickness. Catalytic heating augmentation of the plug materials is assumed to be the same as RCC. The application of NOAX to the edges of the C/SiC cover plate serves to eliminate flow underneath it as well as provide a ramped surface which can mitigate the protuberance heating. NOAX is part of the standard procedures when using the plug repair and an additional factor of 0.84 is applied to the augmented heating when NOAX is used, otherwise a factor of 1.0 is implemented.

Radiant Thermal Models

A set of radiant tests using plug hardware was performed at the Johnson Space Center (JSC) Radiant Heat Test Facility (RHTF) for the purpose of correlating the thermal math model.[2] The test involved exposing a damaged RCC plate repaired with the plug hardware to a radiant heat environment and measuring the thermal response. The test article was mounted to a graphite box which established the boundary conditions for the internal repair hardware representative of the WLE internal environment. A total of 27 thermocouples were installed on the test article, while five fiber optic pyrometers were used to measure the temperatures of the C/SiC inner mold line. A radiometer was used to measure the heat flux output from the heater array. Though the test was predominantly focused on thermal performance, the test series also provided bolt load and gap measurements at operational temperatures further enhancing the confidence in the plug repair.

Two separate thermal models were developed as part of the model correlation effort. The first model represented the calibration test article (i.e. an undamged RCC plate) and the graphite box. This model was intended to ensure that the modeling of the graphite box, tile, and radiant heater was adequate. Particular attention was given to the graphite material properties and contact conditions (e.g. tile to graphite, etc.). The instrumented, undamaged RCC plate was created by an extrusion process, offset from the graphite edge, which allowed the plug test article curvature to be captured without the through-hole. The calibration thermal model is shown in Figure 5 .

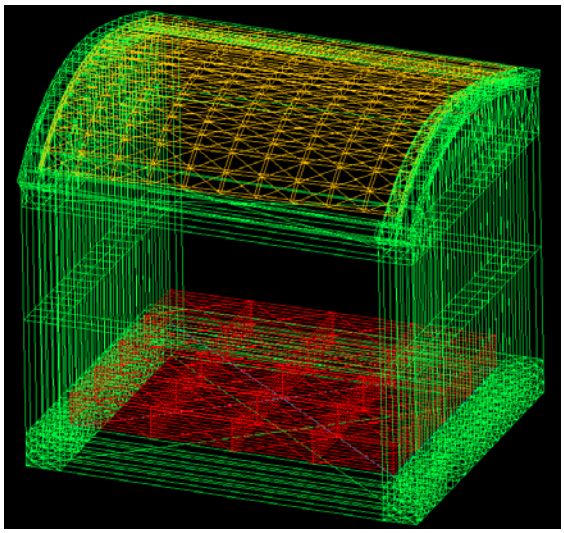

Figure 5: **Radiant Calibration Thermal Model**

The radiometer data from the first plug test article was used to evaluate the final calibration test since the heat flux data gathered during the calibration tests were determined be erroneous. The first plug test provided excellent radiometer data and the power profile and heater performance matched the calibration test. An effective heater temperature was derived from the heat flux measured by the radiometer.

The temperature of the heater is then treated as a boundary condition for radiative transfer to the external OML surfaces of the C/SiC, RCC, and graphite. A node-to-surface conductor was employed to model the radiative heat transfer and assumed grey body radiation and parallel flat plates for the geometry. A separate radiative analysis including the representative heater geometry and test article confirmed that the external radiative modeling simplification was appropriate.

The second radiant test model represented the plug repair test article integrated into the graphite box. The objective of the plug repair test model was to correlate the plug thermal math model. The model, shown in Figure 6, included the RCC plate with a 2 in. hole, C/SiC plug cover plate, TZM attach hardware, graphite box, and tile insulation. The thermal model correlation was accomplished largely by fine tuning the contact conductances until the model matched the test data at the thermocouple locations.

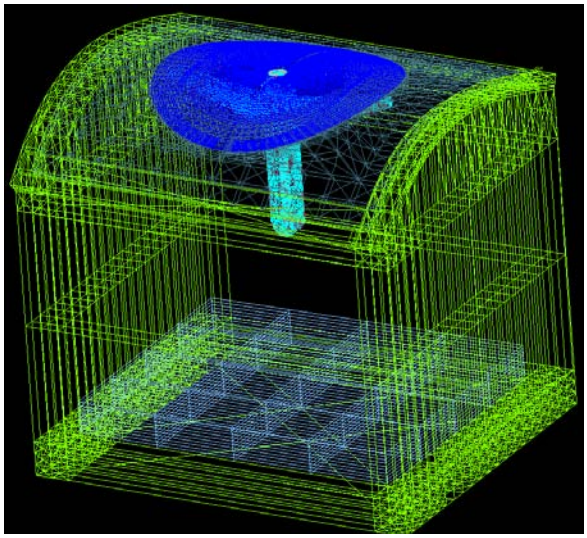

Figure 6: Radiant Plug Thermal Model

As part of the correlation process, test specific changes to the test article model were required. Since thermocouples were grouped and bonded at the base of the housing, the instrumentation effectively blocked any potential backside radiation at the base of the housing. To account for this, the surfaces at the base of the housing were not allowed to radiate to other surrounding surfaces (i.e. surfaces were set to *none* in the radiation analysis). Additionally, the RCC hole was not a clean through hole and some petaling of broken carbon plies could block radiation from the C/SiC directly onto the TZM hardware. Thus, a radiation blocker was included in the model to represent these conditions. The surface was modeled as a 0.012 in. thick surface with a 1 in. sized diameter hole. It was allowed to participate in the radiation analysis.

The data from the first radiant test was used for model correlation. Nodes in the TMM were identified which closely corresponded to the thermocouple locations and compared to the test data. The model was then iterated primarily by varying the contact conductance at eight interfaces. However, since the emissivity for the TZM uncoated surfaces was not well established, it was included as part of the correlation. Model correlation was established with the best fit of the test data. Once the thermal model was correlated, the data from the third radiant test was evaluated to verify the model using a different thermal profile and bolt load conditions.

Radiant Correlation

The plug test article model was correlated to the first radiant Test data by varying the contact conditions and model parameters until the model results agreed with all of the thermocouple responses.

The C/SiC cover plate temperatures were measured via pyrometer. There was a 202°F temperature difference amongst the 5 pyrometer locations plotted in Figure 7. The C/SiC analytical predictions fell within the scatter of the data. At the pyrometer location 4, the peak measured temperature was 2634°F. The model predicted 2538°F, 3.8% below the test data. At the other pyrometer locations, the difference in temperature varied from 2.1 to 3.8%.

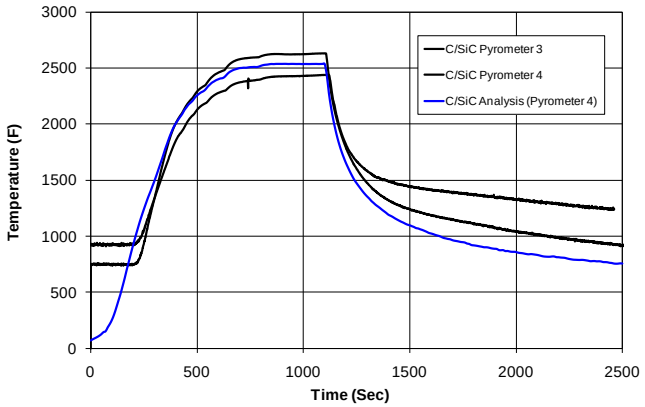

Figure 7: Test 1 Correlated C/SiC Results

The RCC plate temperatures were measured with thermocouples. The correlated model fell between the two available measurements, shown in Figure 8. The peak RCC measured temperature was 2423°F, and the model predicted 2382°F, within 2.1% of the peak measurement.

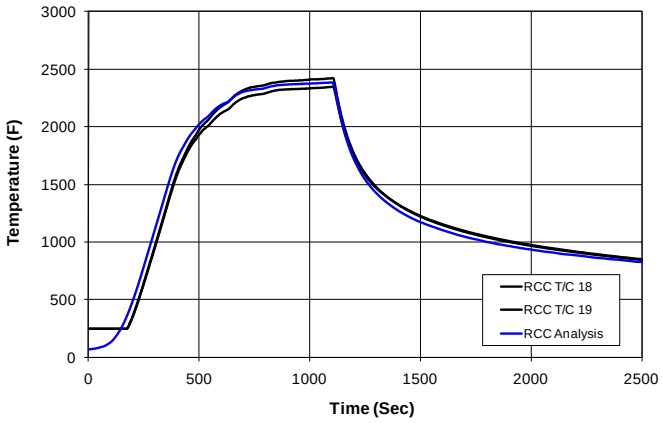

Figure 8: Test 1 Correlated RCC Results

Figure 9 shows the temperature distribution on the TZM hardware at peak temperature prior to the radiant heater shut-off.

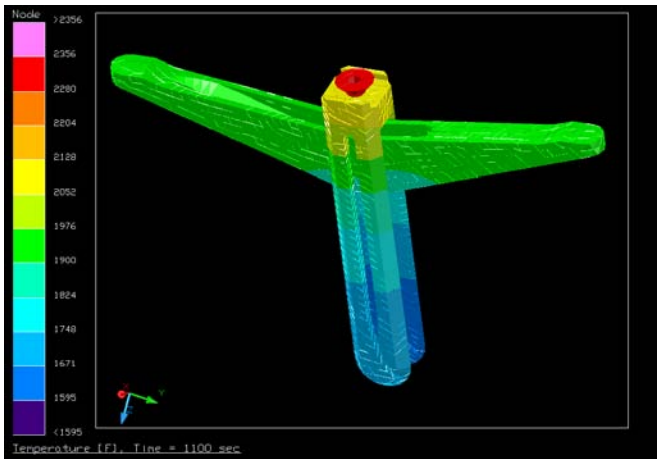

Figure 9: TZM Temperature Distribution

The TZM model correlations are shown in Figure 12-12. The correlated TZM temperatures matched the test data closely at all locations. The largest difference between the test and model was on the bolt, Figure 12, with the model over predicting by 3.6%.

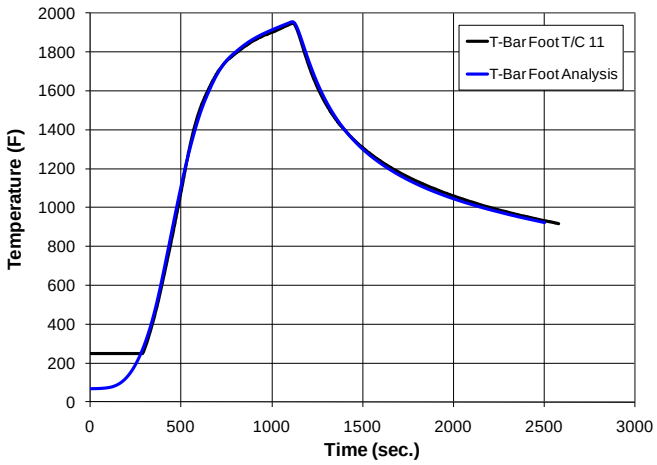

Figure 10: TZM T-Bar Foot Correlation Results

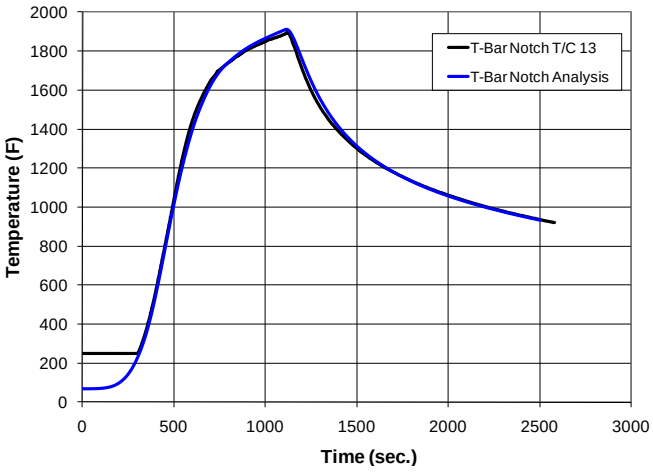

Figure 11: TZM T-Bar Notch Correlation Results

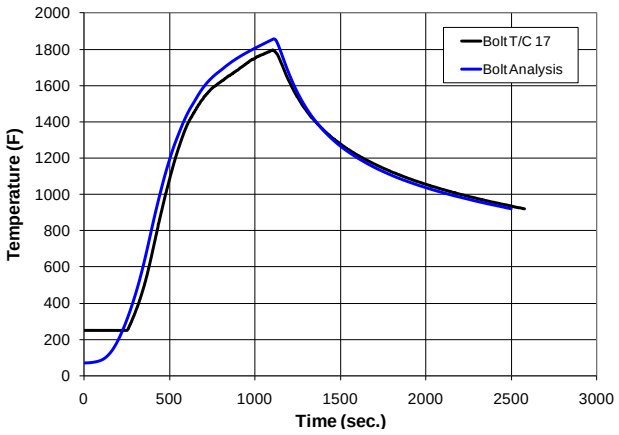

Figure 12: TZM Bolt Correlation Results

The Test 1 correlation summary is listed in Table 1 and contains the model and test comparisons for all of the available test article measurements.

Table 1: Test 1 Correlated TMM Results

Component	Plug TMM Peak Temperature (F)	Test Peak Temperature (F)	% Difference*
C/SiC (Pyrometer 1)	2545	2495	+ 2.1 %
C/SiC (Pyrometer 3)	2534	2443	+ 3.8 %
C/SiC (Pyrometer 4)	2538	2634	- 3.8 %
C/SiC (Pyrometer 5)	2558	2611	- 2.9 %
RCC (T/C 18)	2382	2423	- 2.1 %
RCC (T/C 19)	2385	2348	+ 1.6 %
T-Bar Foot	1956	1946	+ 0.5 %
T-Bar Mid	1912	1868	+ 2.5 %
T-Bar Notch	1912	1893	+ 1.0 %
Bolt	1856	1795	+ 3.6 %
Housing	1779	1757	+ 1.3 %

***% Difference calculated:** $(T_{model} - T_{test})/(T_{test} - T_{initial})$

Based on the model correlation, several changes were incorporated into the real-time mission support model. Some of the additions had minor effects while others had significant effects on the model correlation. The bolt thread emissivity was increased to 0.85 to best match the test data and had a significant effect. The physical rationale for increasing the emissivity, relative to a smooth uncoated TZM surface, is due to the highly irregular threaded surface, which can have the effect of trapping heat, and the effect of the lubricant material burning at slightly elevated temperatures and leaving a black residue. Small adjustments to the emissivity for IML C/SiC and TZM uncoated surfaces were made based on the correlation with values of 0.82 and 0.3, respectively. A change was made to the bolt conductivity to correct for the bolt geometry in the model. A constant cross section was assumed for the bolt and, thus, the model did not account for the threaded region. A factor of 0.68 was applied to the thermal conductivity in the threaded region to account for the reduction in effective area. The inclusion of the factor on the bolt thread conductivity, however, had only a minor effect on the results.

The final correlated contact conductances and other model parameters derived from the first radiant test were not altered to analyze the third test, which had a different thermal profile and bolt load. The comparison of the analysis and test results showed similar agreement as seen with the first set of test data. The test data and analysis varied between 1.5 to 3.2% with the analysis always over predicting the peak test temperature.

Flight Design Reference Cases

The correlated plug repair thermal model was then evaluated with the heating environments from the flight DRCs to ensure that the material temperature limits are not exceeded and provide thermal loads to the thermo-structural analysis. The established temperatures limits in an oxidizing environment for C/SiC, RCC, and TZM are 3450°F, 3220°F, and 3133°F, respectively.[6],[7],[8] PHAT v2.3 was used with the ISSHVFW trajectory heating parameters. Figure 13 shows the distribution of temperatures for the Panel 9 BP5505 DRC at 870 seconds into the profile.

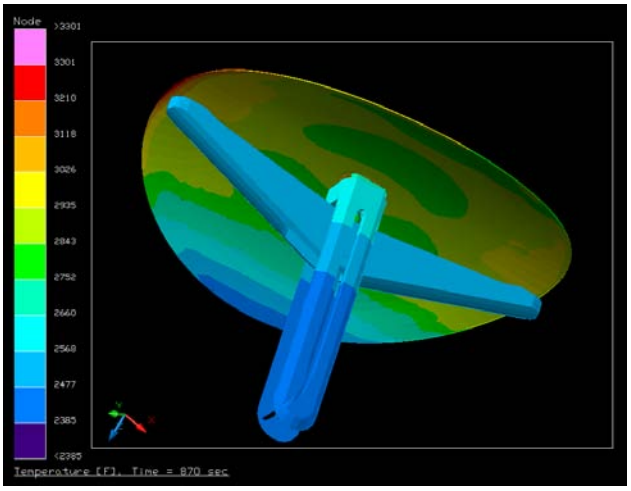

Figure 13: BP5505 DRC Temperature Distribution at 870 sec.

The results from each of the DRCs are summarized in Table 2.

Table 2: Results of Flight Design Reference Case Analyses for 0.020 in. Gap Height

Component	BP5505 DRC		Panel 8 Zone 2 DRC		BP5951 DRC	
	Peak Temperature (F)	Time @ Peak Temperature (sec.)	Peak Temperature (F)	Time @ Peak Temperature (sec.)	Peak Temperature (F)	Time @ Peak Temperature (sec.)
C/SiC (Plug Edge)	3704*	1000	2974	950	2591	850
RCC (Plug Edge)	3062	800	2776	810	2485	830
Bolt Head	3126	800	2862	810	2222	860
T-Bar Foot	2557	860	2552	860	2047	940
T-Bar Notch	2543	860	2555	860	2038	940
Housing	2667	850	2611	840	2079	910
Barrel Nut	2550	860	2562	860	2045	940

**exceeds C/SiC material temperature limit, 3450°F*

An exceedance of the C/SiC temperature limit is predicted for the BP5505 DRC at the plug edge with a 0.020 in.gap. A small region at the forward edge of the C/SiC cover plate exceeds the 3450°F temperature limit by 254°F as shown in Figure 14. As a means of comparison, arc jet testing was performed on full scale plug repair specimens for the BP5505 DRC with 0.020 in. plug edge gaps[9]. The plug repair survived the entire 1200 sec. exposure and the infrared data yielded peak temperatures of ~3500°F at the leading edge of the plug. While still below the 3700°F analytical prediction presented here, the test temperatures were indeed slightly larger than the material limit and post-test evaluation did show some minute erosion. The analytical predictions may be conservative due to the application of bump factors attributed to the application of NOAX, but overall, the analytical predictions are still consistent with the observations from arc jet testing.

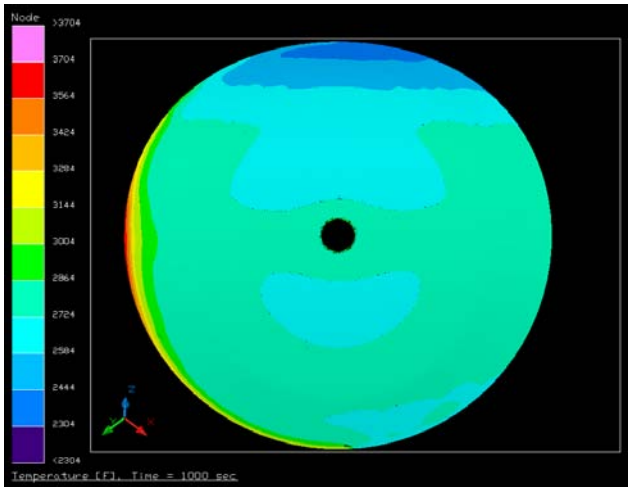

Figure 14: C/SiC Peak Temperature Distribution at BP5505 DRC with 0.020 inch Gap.

The C/SiC temperature limit was evaluated for the BP5505 DRC with smaller gap heights. Gap heights of 0.000, 0.005, and 0.010 in. at the edge facing the flow direction were analyzed. Recall, the analysis assumes that the plug edge thickness is at the max tolerance value of 0.025 in. Figure 15 shows the peak temperature location at the small local area, which is protected by NOAX. The results show that the forward edge of the cover plate needs to have a gap less than 0.005 in order to stay below the C/SiC temperature limit.

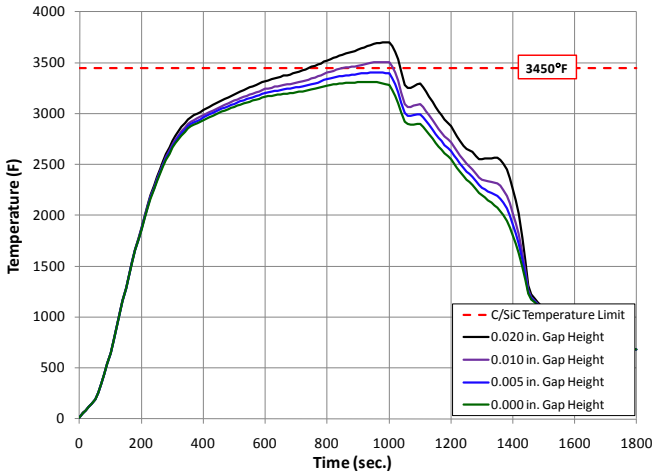

Figure 15: C/SiC Temperatures for Varying Plug Edge Gap Heights (BP5505 DRC)

Clearly, the application of NOAX on the edge of the plug is required for the repair to survive at the Panel 9 BP5505 DRC. However, for the Panel 8 Zone 2 DRC and more benign environments, the use of NOAX is not necessary. Table 3 shows that while NOAX serves to decrease the plug edge temperatures, the temperatures at the Panel 8 Zone 2 DRC remain below the C/SiC temperature limits even without the application of NOAX for gap sizes up to 0.020 inches.

Table 3: Panel 8 Zone 2 DRC C/SiC Sensitivity to NOAX

Plug Edge Gap Size (in.)	Peak Temperature with NOAX (°F)	Peak Temperature without NOAX (°F)
0.000	2839	2919
0.010	2898	2994
0.020	2974	3101

The bolt head temperature should be lower than predicted since the bolt is not heated directly. There is a layer of NOAX above the bolt to reduce the potential for oxidation.

The influence of hole size on the resulting peak temperatures was assessed with the BP5505 DRC with a 0.020in. edge gap. The largest temperature difference identified was 7°F on the housing between the 4 in. and 2 in. hole.

Conclusions

A thermal math model for the RCC plug repair was developed to increase the confidence in the repair entry performance and provide a real-time mission support tool. The thermal response of the plug cover plate, local RCC, and TZM attach hardware can be assessed with the model. The geometry and spatial location of the mesh also matches the structural model which allows for the direct mapping of temperature loads onto the structural model. The model was correlated to the full scale plug repair radiant test. Three DRCs were evaluated with the correlated plug thermal math model. The Panel 8 Zone 2 and BP5951DRCs did not exceed any temperature limits with a 0.020 in. gap and no NOAX applied to the plug leading edge. The BP5505 DRC required a gap less than 0.005 in and the application of NOAX to maintain temperatures below the failure temperature of the C/SiC cover plate.

References

1. **Sapayo, Jacob and Hernandez, Marc.** *Thermal Analysis of RCC Repair Flexible Plug Design.* ATK Thiokol. June 2005. TR015872.
2. **Rodriguez, Alvaro C.** *RCC Plug Repair Radiant Test.* April 2009. JSC-64870.
3. **Anderson, Brian.** *RCC Repair Design Reference Cases in Support of NOAX and Plug Repairs.* April 2007. EG-SS-07-03.
4. *Post-Test report for Aerothermal Wind Tunnel Verification Test OH-200: RCC Repair C/SiC Plug and*

NOAX Crack Repair Model Configurations (Model 204-0). May 2007. SE07HB008.
5. **Marek, Lindsey and Anderson, Brian.** *RCC Protuberance Test Engineering Correlation Development.* November 2009. Aeroheating Panel Presentation.
6. **Rodriguez, Alvaro.** *RCC Plug Repair C/SiC Material Evaluation Arc Jet Test Phase II.* February 2009. JSC-64660.
7. *Space Shuttle Program Thermal Analysis Data Book OV-103 Performance Enhancement Revision A Volume 1 of 31.* May 1997. SSD95D0405-A.
8. **Davis, Andrew.** *Arc Jet Testing of Low Temperature Processed R512E TZM Coatings (Orbiter RCCR).* ATK Thiokol. July 2005. TR016037.
9. **Lester, Dean.** *Final Report for Reinforced Carbon-Carbon Plug Repair Flight Type Test Article Arc Jet Test IHF 177.* September 2006. TR018045.